

## Measurement of top quark polarization in the lepton+jets final state

The DØ Collaboration  
(Dated: September 11, 2015)

We present a measurement of the top quark polarization in the  $t\bar{t}$  pair production in  $p\bar{p}$  collisions at the Fermilab Tevatron collider at  $\sqrt{s} = 1.96$  TeV. We use the full Run II data sample corresponding to  $9.7 \text{ fb}^{-1}$  of integrated luminosity recorded with the DØ detector. We consider the final state containing a lepton (electron or muon) and at least three jets. The polarization is measured through the distribution of lepton angles. We consider three different axes for the polarization measurement: the beam axis, the helicity axis, and the axis normal to the  $t\bar{t}$  production plane. This is the first measurement of the transverse polarization of the top quark at a hadron collider. The observed top quark polarizations for each of the three axes are consistent with standard model predictions of nearly zero polarization.

*Preliminary Results for Summer 2015 Conferences*

The top quark was discovered at the Tevatron collider [1, 2] and plays an important role in particle physics because of its unique properties. It is the heaviest known elementary particle with  $m_t = 173.34 \pm 0.76$  GeV [3], and it has a very short lifetime of about  $5 \times 10^{-25}$  s [4]. The standard model (SM) predicts that top quark pairs are produced almost unpolarized at the Tevatron (a small longitudinal polarization is generated by SM parity-violating weak interactions [5]), while various models beyond the standard model (BSM) predict non-zero polarization of the top quark pairs. The transverse polarization is allowed in strong interaction processes and is therefore predicted non-zero in the SM. The top quark polarization  $P_{\hat{n}}$  can be measured in the top quark rest frame through the angular distribution of the top quark decay products with respect to a chosen axis  $\hat{n}$  [5, 6]:

$$\frac{1}{\Gamma} \frac{d\Gamma}{d \cos \theta_{i,\hat{n}}} = \frac{1}{2} (1 + P_{\hat{n}} \kappa_i \cos \theta_{i,\hat{n}}), \quad (1)$$

where  $i$  is the decay product (lepton, quark, neutrino),  $\kappa_i$  its spin analyzing power ( $\approx 1$  for lepton, 0.97 for  $d$ -type quark,  $-0.4$  for  $b$ -quark, and  $-0.3$  for neutrino and  $u$ -type quark [6, 7]), and  $\theta_{i,\hat{n}}$  is the angle between the direction of the decay product  $i$  and the quantization axis  $\hat{n}$ . The quantization axis is obtained after a boost to the  $t\bar{t}$  rest frame, while the decay product directions are obtained after successively boosting the particles to the  $t\bar{t}$  rest frame and then to the parent top rest frame. Here we measure the polarization with three choices of spin quantization axis:

- the **beam axis**  $\hat{b}$ , given by the direction of the proton beam,
- the **helicity axis**  $\hat{h}$ , given by the direction of the parent top quark,
- the **transverse axis**  $\hat{t}$ , given as perpendicular to the production plane defined by the proton and parent top quark directions. The positive  $\hat{t}$  axis is given by cross product  $\hat{p}(p) \times \hat{p}(t)$  [8, 9].

The top quark polarization along the helicity axis was previously studied in  $p\bar{p}$  collisions by the D0 Collaboration [10] as part of the leptonic asymmetries measurement. Recently, the D0 Collaboration measured top quark polarization along the beam axis, simultaneously with the forward-backward asymmetry in the  $t\bar{t}$  final states with two leptons [11]. The observations from both measurements are consistent with the SM. The ATLAS and CMS Collaborations measured the top quark polarization in  $pp$  collisions in the helicity basis and the results are consistent with zero polarization [12, 13]. The Tevatron and the LHC polarizations are expected to be different due to the difference in the initial states. There is a strong motivation [14] from the theoretical point of view to measure both longitudinal and transverse polarization in the Tevatron data.

The SM predictions for the longitudinal top quark polarization at the Tevatron are  $-0.19 \pm 0.05\%$  in the beam basis and  $-0.39 \pm 0.04\%$  in the helicity basis [15]. The transverse top quark polarization is estimated to be 1.1% at the Tevatron [8]. Observation of significantly non-zero longitudinal top quark polarization would be clear evidence for BSM physics [6, 16].

In this note, we present a measurement of the top quark polarization in the lepton+jets final state of  $t\bar{t}$  production at the Tevatron collider. As discussed above, the lepton is the most sensitive to the top quark polarization and is the most easily identified final state fermion. Therefore this measurement focuses on studying the angular distribution of leptons. After selecting the events in the lepton+jets final state, we perform a kinematic fit to reconstruct the lepton angles. The resulting angular distributions are fitted with mixtures of signal templates of polarization  $+1$  and  $-1$  to measure the polarization. The down-type quark has also analyzing power close to unity, but its identification is difficult and thus not used to measure the top quark polarization. However, the down-type quarks from Monte Carlo simulations are used to produce the signal templates as described below.

We analyze data collected by the D0 detector corresponding to an integrated luminosity of  $9.7 \text{ fb}^{-1}$  of  $p\bar{p}$  collisions at  $\sqrt{s} = 1.96$  TeV. The D0 detector central-tracking system consists of a silicon microstrip tracker and a central fiber tracker, both surrounding the interaction region for pseudorapidities <sup>1</sup>  $|\eta_d| < 3$  and  $|\eta_d| < 2.5$ . The central-tracking system, located within a 1.9 T superconducting solenoidal magnet [17, 18], provides measurements for tracking and vertexing. A liquid-argon calorimeter with uranium absorber plates has a central section covering pseudorapidities up to  $|\eta_d| \approx 1.1$ , and two end calorimeters that extend coverage to  $|\eta_d| \approx 4.2$ , with all three housed in separate cryostats [19]. An outer muon system, at  $|\eta_d| < 2$ , consists of a layer of tracking detectors and scintillation trigger counters in front of 1.8 T iron toroids, followed by two similar layers after the toroids [20].

---

<sup>1</sup> The pseudorapidity  $\eta_d = -\ln[\tan(\theta/2)]$  is measured relative to the center of the detector, and  $\theta$  is the polar angle with respect to the proton beam direction.

The top quark decays into a  $b$  quark and a  $W$  boson with approximately 100% probability resulting in a  $W^+W^-b\bar{b}$  final state. This analysis is performed using the lepton + jets final state, where one of the  $W$  bosons decays leptonically and the other hadronically. Here, lepton denotes either an electron ( $e$ ) or a muon ( $\mu$ ), including those from leptonic tau decays of the  $W$  boson. This analysis requires the presence of one isolated electron [21] or muon [22] with transverse momentum  $p_T > 20$  GeV and  $|\eta| < 1.1$  or  $|\eta| < 2$ , respectively. In addition, leptons are required to originate from the  $p\bar{p}$  interaction vertex (PV) by demanding  $|\Delta z(\ell, \text{PV})| < 1$  cm. Accepted events must have a reconstructed PV within 60 cm of the center of the detector along the beam axis. Furthermore, we require missing transverse momentum  $\cancel{p}_T > 20$  GeV that is expected from the undetected neutrino. Jets are reconstructed using an iterative cone algorithm [23] with a cone parameter of  $R = \sqrt{\Delta\eta^2 + \Delta\phi^2} = 0.5$ , where  $\phi$  is the azimuthal angle around the proton beam direction. Jet energies are corrected to the particle level using calibrations derived from exclusive  $\gamma$ +jet,  $Z$ +jet, and dijet events [24]. These calibrations account for differences in detector response to jets originating from a gluon, a  $b$  quark, and  $u, d, s$ , or  $c$  quarks. We require at least three jets with  $p_T > 20$  GeV within  $|\eta| < 2.5$ , and  $p_T > 40$  GeV for the jet of highest  $p_T$ . At least one jet per event is required to be identified as originating from a  $b$  quark ( $b$ -tagged) through the use of a multivariate algorithm [25]. For the  $\mu$ +jets sample upper limits on the transverse mass of the reconstructed  $W$  boson of  $M_T^W < 250$  GeV and  $\cancel{p}_T < 250$  GeV are applied to remove events in data with misreconstructed muon  $p_T$ . Additional selection requirements are applied in order to reduce misreconstructed muon  $p_T$  events further and also to suppress background contributions from multijet production. Those requirements can be found in Ref. [26], where the same selection criteria are applied. The number of events obtained after the final selection is shown in Table I.

We use Monte Carlo simulated  $t\bar{t}$  events generated using the MC@NLO event generator version 3.4 [27] or the ALPGEN event generator version 2.11 [28]. Parton showering, hadronization, and underlying event modeling are performed with HERWIG [29] for MC@NLO events and with PYTHIA [30] for ALPGEN events. The detector is simulated using GEANT3 [31]. The main background to  $t\bar{t}$  production is  $W$ +jets production, where one  $W$  boson is produced via an electroweak interaction together with additional partons from QCD processes. The  $W$ +jets final state can be split into four subsamples according to parton flavor:  $Wb\bar{b}$ +jets,  $Wc\bar{c}$ +jets,  $Wc$ +jets and  $W$ +light jets, where light refers to gluons,  $u$ ,  $d$  or  $s$  quarks. The  $W$ +jets background is modeled with ALPGEN+PYTHIA [28, 30], as are the  $Z$ +jets background events. Other backgrounds include  $WW$ ,  $WZ$  and  $ZZ$  diboson production simulated by PYTHIA and single top electroweak production simulated by COMPHEP [32]. The multijet background, where a jet is misidentified as an isolated lepton, is extracted from the data [26, 33].

A  $\chi^2$ -based constrained kinematic fit is utilized to associate the observed leptons and jets with the individual top quarks as described in [34]. The kinematic fit algorithm includes a technique that allows reconstruction of events with lepton and three jets, *i.e.* when one jet is lost, typically because the jet is too soft or because of inefficiencies in reconstruction and identification [35]. The three-jet event kinematic fit performance is comparable to that for the four-jet events. The addition of the three-jet sample to the four-jet sample almost doubles the number of top quark events, as reported in Ref. [37], where the same kinematic fit was used on the same dataset. For the measurement, all possible combinations of objects are considered and weighted by the  $\chi^2$  of the kinematic fit solution and the  $b$ -tagging probability. For the event selection, we used the reconstructed kinematic variables corresponding to the combination with the best  $\chi^2$ .

To determine the sample composition we choose input variables that form a kinematic discriminant based on the approximate likelihood ratio between the  $t\bar{t}$  and  $W$ +jets predictions. The input variables are selected for good separation between the  $t\bar{t}$  events and the  $W$ +jets events. The input variables are required to be well modeled and not strongly correlated with one another or to the lepton polar angles used for the measurement. The input variables for the lepton and exactly three jet ( $\ell + 3$  jet) and the lepton and four or more jets ( $\ell + \geq 4$  jet) samples are chosen independently. The  $\ell + 3$  jet and  $\ell + \geq 4$  jet samples are each divided into 3 sub-channels according to the number of  $b$ -tagged jets: 0, 1,  $\geq 2$ . The zero- $b$ -tag channels are used only to determine the sample composition and background calibration, not to measure the polarization.

The input variables used for the  $\ell + 3$  jet discriminant are:

- $k_T^{\min} = \min(p_{T,a}, p_{T,b}) \cdot \Delta R_{ab}$ , where  $\Delta R_{ab} = \sqrt{(\eta_a - \eta_b)^2 + (\phi_a - \phi_b)^2}$  is the angular distance between the two closest jets,  $a$  and  $b$ , and  $\min(p_{T,a}, p_{T,b})$  represents the smaller transverse momentum of the two jets;
- aplanarity,  $A = 3/2\lambda_3$ , where  $\lambda_3$  is the smallest eigenvalue of the normalized momentum tensor  $M_{i,j}$ ;
- $H_T^\ell$ , the scalar sum of the jets and lepton transverse momenta;
- $\Delta\mathcal{R}(\text{jet1}, \text{jet2})$ ,  $\Delta\mathcal{R}$  between the leading jet and the second leading jet;
- $\Delta\mathcal{R}(\text{lepton}, \text{jet1})$ ,  $\Delta\mathcal{R}$  between the lepton and the leading jet.

The input variables used for the  $\ell + \geq 4$  jet discriminant are:

- $k_T^{min}$ ;
- aplanarity;
- $H_T^l$ ;
- centrality,  $C = H_T/H$ , where  $H_T$  is the scalar sum of all jet transverse momenta and  $H$  is the scalar sum of all jet energies.
- the lowest  $\chi^2$  of the different kinematic fit solutions;
- $(p_T^{b_{had}} - p_T^{b_{lep}})/(p_T^{b_{had}} + p_T^{b_{lep}})$ , the relative asymmetry of the transverse momenta of the two  $b$ -jet candidates, where  $b_{lep}$  is from the top quark that decays to  $b\ell\nu$  and  $b_{had}$  is from the top quark that decays to  $bq\bar{q}'$ ;
- $M_{jj}$ , the invariant mass of the jets corresponding to the  $W \rightarrow q\bar{q}'$  decay.

The sample composition is determined from a simultaneous maximum-likelihood fit to the discriminant distribution for the  $t\bar{t}$  signal and  $W$ +jets background. The  $W$ +jets background is normalized separately for the heavy-flavor contribution ( $Wb\bar{b}$  + jets and  $Wc\bar{c}$  + jets) and for the light parton contribution ( $Wc$  + jets and  $W$ +light jets). The sample composition after selection and after fit and its breakdown into individual channels by lepton flavor and number of jets are summarized in Table I.

Source	3 jets		$\geq 4$ jets	
	$e$ +jets	$\mu$ +jets	$e$ +jets	$\mu$ +jets
$W$ +jets	$1741 \pm 26$	$1567 \pm 15$	$339 \pm 3$	$295 \pm 3$
Multijet	$494 \pm 7$	$128 \pm 3$	$147 \pm 4$	$49 \pm 2$
Other Bg	$446 \pm 5$	$378 \pm 2$	$87 \pm 1$	$73 \pm 1$
$t\bar{t}$ signal	$1200 \pm 25$	$817 \pm 20$	$1137 \pm 24$	$904 \pm 23$
Sum	$3881 \pm 37$	$2890 \pm 25$	$1710 \pm 25$	$1321 \pm 23$
Data	3872	2901	1719	1352

TABLE I: Estimated number of events after selection (including requirement of at least one jet being  $b$ -tagged) and after determination of the sample composition from maximum-likelihood fit to the discriminant distribution as discussed in text. The quoted uncertainties are statistical.

Once the sample composition is known and the full reconstruction is done, we need the lepton angular distributions for the  $W$ +jets events to be properly modeled, so it does not bias the final template fit. The  $W$ +jets events are the leading background and are especially important in  $\ell$ +3 jet sample. To obtain a good model of the  $W$ +jets templates, we use the data in the  $\ell$ +3 jets and 0  $b$ -tag control sample, which is dominated by the  $W$ +jets background with more than 70% contribution. This sample is not used for the polarization measurement. The  $t\bar{t}$  events and other background components are subtracted from data. We reweight the  $W$ +jets MC events so that the  $\cos\theta_{\ell,\hat{n}}$  distribution shows good agreement with the data. The correction obtained in the control sample is propagated to the other samples. We do not require any specific correction for the other background sources as their contributions are under 10% (second largest is multijet background, see Table I) and this correction would add another source of systematic uncertainty.

To measure polarization, a template fit to the reconstructed lepton  $\cos\theta_{\hat{n}}$  distribution is made. The  $t\bar{t}$  MC sample is only generated with zero polarization. We then obtain two templates of +1 and -1 polarization by reweighting the simulated  $t\bar{t}$  events based on the double differential distribution:

$$\frac{1}{\Gamma} \frac{d\Gamma}{d\cos\theta_1 d\cos\theta_2} = \frac{1}{4} (1 + \kappa_1 P_{\hat{n},1} \cos\theta_1 + \rho\kappa_2 P_{\hat{n},2} \cos\theta_2 - \kappa_1\kappa_2 C \cos\theta_1 \cos\theta_2), \quad (2)$$

where index 1 represents the top decay product (lepton or down-type quark as they have the largest spin-analyzing power) and index 2 the anti-top decay product,  $\kappa$  is the spin-analyzing power and  $C$  stands for the anti-correlation factor, representing the spin correlation of the  $t\bar{t}$  pair. We use the SM values  $C = -0.368$  (helicity axis) and  $C = 0.791$  (beam axis), both calculated at next to leading order in QCD and electroweak couplings [5]. The spin correlation factor is not known for the transverse axis and we set  $C = 0$ .  $P_{\hat{n},i}$  represents the polarization state we want to reweight to (here  $P_{\hat{n},i} = \pm 1$ ) along the chosen axis  $\hat{n}$ . In the SM with  $CP$  invariance, the relative sign factor  $\rho$  takes the value +1 for the helicity basis and -1 for the beam and transverse bases [5, 36].

A simultaneous fit is performed to the data using the  $P = +1$  and  $-1$  signal templates and the background template normalized to the expected background contribution. The fit is simultaneously made for the eight samples defined according to the lepton flavor ( $e$  or  $\mu$ ), lepton charge and number of jets (3 or  $\geq 4$ ). The observed polarization is taken as  $P = f_+ - f_-$ , where  $f_{\pm}$  are the fractions of  $P = +1$  and  $-1$  returned in the fit. The fit and the method are verified by an ensemble testing procedure with 1000 ensembles for five polarization values. The distributions of the cosines of the polar angles of leptons from  $t\bar{t}$  decay for all three axes are shown in Fig. 1.

A simultaneous measurement of the top quark polarization and the forward-backward asymmetry in the dilepton final states [11] observed a correlation between the two measurements. This correlation is due to acceptance and resolution effects in the event kinematic reconstruction. We determine the dependence of the observed polarization on the parton level forward-backward asymmetry,  $A_{FB}$ , from samples in which the  $t$  and  $\bar{t}$  rapidity distributions are reweighted. We perform a correction for the difference between the nominal MC@NLO production-level  $A_{FB}$  of  $(5.01 \pm 0.03)\%$  and the NNLO calculation [38] of  $(9.5 \pm 0.7)\%$ . The observed correction is  $-3.0\%$  for the polarization along the beam axis, less than  $0.2\%$  for the polarization along helicity axis and negligible for the transverse polarization. The uncertainty on the forward-backward asymmetry prediction is propagated to the measurement as a systematic uncertainty.

Three categories of systematic uncertainties are evaluated using fully simulated events including background contributions: modeling of signal and background events, uncertainties in the simulation of the detector response, and uncertainties associated with procedures used and assumptions made in the analysis. The sources of systematic uncertainties and their contributions are listed in Table II. The alternate signal uncertainty is computed from the difference between the nominal MC@NLO and ALPGEN+PYTHIA generators and contains the contributions from both hadronization and higher order corrections. More details about the methodology of systematic uncertainty determination can be found in [37].

Source	Beam	Helicity	Transverse
<i>Signal and background modeling:</i>			
Alternate signal	$\pm 0.009$	$\pm 0.014$	$\pm 0.003$
Initial/final state radiation	$\pm 0.008$	$\pm 0.003$	$\pm 0.003$
Color reconnection	$\pm 0.003$	$\pm 0.007$	$\pm 0.003$
Multijet background	$\pm 0.001$	$\pm 0.008$	$\pm 0.002$
Background normalization	$\pm 0.004$	$\pm 0.003$	$\pm 0.002$
$b$ -jet fragmentation	$\pm 0.001$	$\pm 0.001$	$\pm 0.000$
PDF uncertainty	$\pm 0.013$	$\pm 0.011$	$\pm 0.003$
Top quark mass	$\pm 0.002$	$\pm 0.005$	$\pm 0.003$
Instantaneous luminosity	$\pm 0.000$	$\pm 0.002$	$\pm 0.002$
<i>Detector modeling:</i>			
Residual jet energy scale	$\pm 0.009$	$\pm 0.022$	$\pm 0.003$
Flavor-dependent jets response	$\pm 0.009$	$\pm 0.008$	$\pm 0.007$
$b$ -tagging	$\pm 0.009$	$\pm 0.014$	$\pm 0.005$
Trigger efficiency	$\pm 0.002$	$\pm 0.005$	$\pm 0.001$
Lepton momentum scale	$\pm 0.002$	$\pm 0.008$	$\pm 0.001$
$t\bar{t}$ transverse momentum	$\pm 0.005$	$\pm 0.001$	$\pm 0.002$
Jet energy resolution	$\pm 0.003$	$\pm 0.005$	$\pm 0.005$
Jet identification efficiency	$\pm 0.001$	$\pm 0.004$	$\pm 0.003$
Lepton identification	$\pm 0.006$	$\pm 0.016$	$\pm 0.002$
Vertex confirmation	$\pm 0.004$	$\pm 0.002$	$\pm 0.004$
<i>Method:</i>			
$W$ +jets calibration	$\pm 0.002$	$\pm 0.003$	$\pm 0.001$
Sample composition	$\pm 0.012$	$\pm 0.007$	$\pm 0.004$
MC template statistics	$\pm 0.001$	$\pm 0.001$	$\pm 0.001$
$A_{FB}$ uncertainty	$\pm 0.005$	$\pm 0.000$	$\pm 0.000$
<i>Total systematic uncertainty</i>	$\pm 0.030$	$\pm 0.041$	$\pm 0.015$
<i>Total statistical uncertainty</i>	$\pm 0.046$	$\pm 0.044$	$\pm 0.030$
<i>Total uncertainty</i>	$\pm 0.055$	$\pm 0.060$	$\pm 0.034$

TABLE II: Summary of uncertainties on the measured top quark polarization along three axes. The numbers indicate difference in polarization when the measurement is repeated using the respective alternative model or after applying uncertainties from the methods or assumptions made in the measurement.

The final measured polarizations for the three spin quantization bases are shown in Table III.

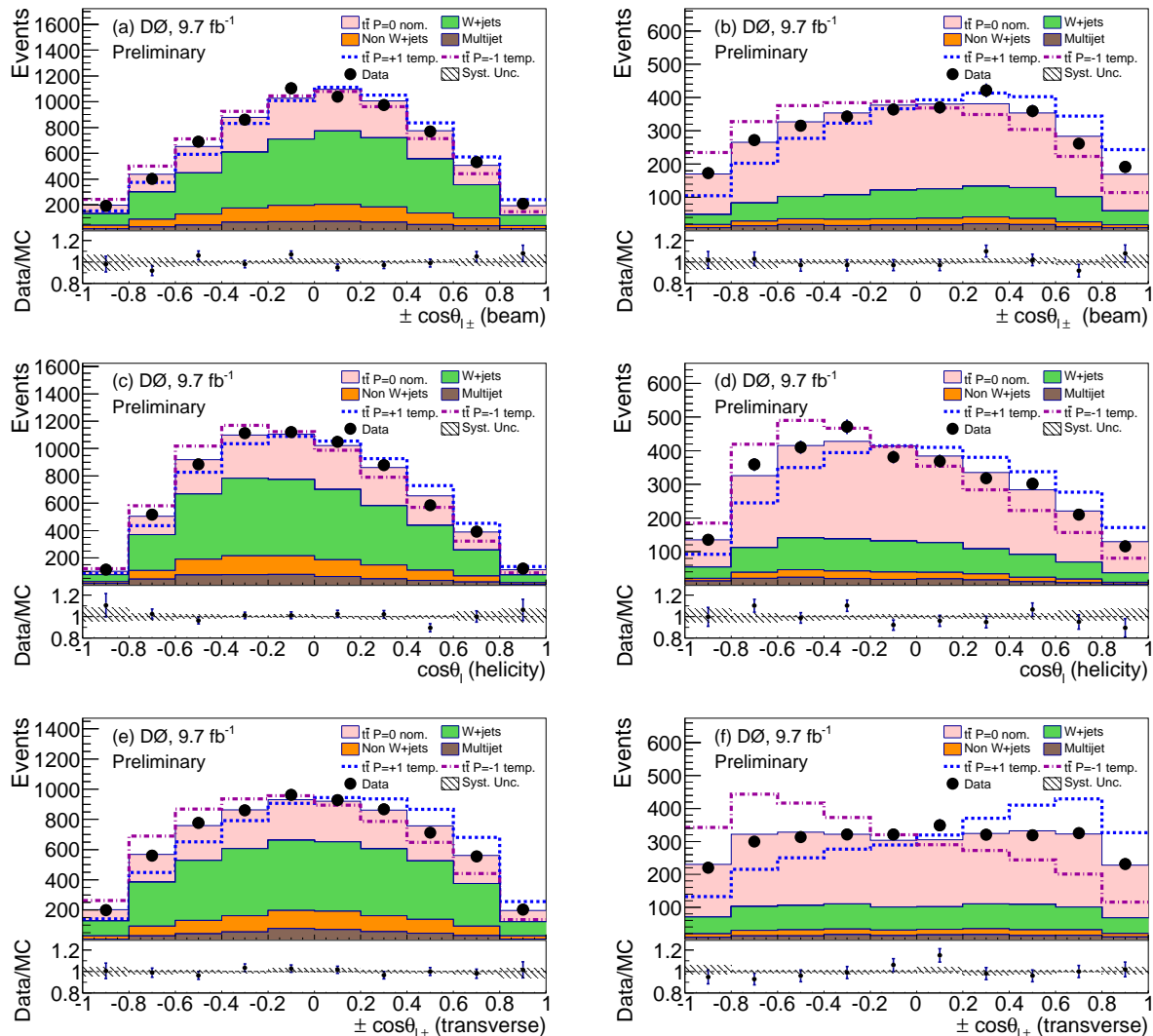


FIG. 1: The combined  $e$ +jets and  $\mu$ +jets  $\cos\theta$  distributions for data, expected backgrounds and signal templates for  $P = -1, 0$  and  $+1$ . Panels (a), (c), and (e) represent selection with exactly three jets. (b), (d), and (f) represent selection with four or more jets. (a) and (b) show distributions in beam axis. (c) and (d) show distributions in helicity axis. (e) and (f) show distributions in transverse axis. The hashed area represents systematic uncertainty. Note that the direction of the  $x$ -axis is changed for the  $\ell^-$  events along beam and transverse axis.

Axis	Measured polarization $P_n$	SM prediction
Beam	$+0.070 \pm 0.055$	$-0.002$
Helicity	$-0.102 \pm 0.060$	$-0.004$
Transverse	$+0.040 \pm 0.034$	$+0.011$

TABLE III: Measured top quark polarization in beam, helicity, and transverse spin quantization bases. The total uncertainties (statistical + systematic) are shown.

Our measured top quark polarizations are consistent with zero and with the predicted SM values. The polarization along the transverse axis has been measured for the first time at a hadron collider and the longitudinal polarization results are the most precise results based on  $p\bar{p}$  collisions.

We thank the staffs at Fermilab and collaborating institutions, and acknowledge support from the Department of Energy and National Science Foundation (United States of America); Alternative Energies and Atomic Energy Commission and National Center for Scientific Research/National Institute of Nuclear and Particle Physics (France);

Ministry of Education and Science of the Russian Federation, National Research Center “Kurchatov Institute” of the Russian Federation, and Russian Foundation for Basic Research (Russia); National Council for the Development of Science and Technology and Carlos Chagas Filho Foundation for the Support of Research in the State of Rio de Janeiro (Brazil); Department of Atomic Energy and Department of Science and Technology (India); Administrative Department of Science, Technology and Innovation (Colombia); National Council of Science and Technology (Mexico); National Research Foundation of Korea (Korea); Foundation for Fundamental Research on Matter (The Netherlands); Science and Technology Facilities Council and The Royal Society (United Kingdom); Ministry of Education, Youth and Sports (Czech Republic); Bundesministerium für Bildung und Forschung (Federal Ministry of Education and Research) and Deutsche Forschungsgemeinschaft (German Research Foundation) (Germany); Science Foundation Ireland (Ireland); Swedish Research Council (Sweden); China Academy of Sciences and National Natural Science Foundation of China (China); and Ministry of Education and Science of Ukraine (Ukraine).

- 
- [1] S. Abachi *et al.* (D0 Collaboration), “Observation of the top quark,” *Phys. Rev. Lett.* **74**, 2632 (1995).
- [2] F. Abe *et al.* (CDF Collaboration), “Observation of top quark production in  $\bar{p}p$  collisions,” *Phys. Rev. Lett.* **74**, 2626 (1995).
- [3] (ATLAS and CDF and CMS and D0 Collaborations), “First combination of Tevatron and LHC measurements of the top-quark mass,” arXiv:1403.4427 [hep-ex].
- [4] V. M. Abazov *et al.* (D0 Collaboration), “An Improved determination of the width of the top quark,” *Phys. Rev. D* **85**, 091104 (2012).
- [5] W. Bernreuther and Z. -G. Si, “Distributions and correlations for top quark pair production and decay at the Tevatron and LHC,” *Nucl. Phys. B* **837** (2010) 90.
- [6] D. Krohn, T. Liu, J. Shelton and L. -T. Wang, “A Polarized View of the Top Asymmetry,” *Phys. Rev. D* **84** (2011) 074034.
- [7] A. Brandenburg, Z. G. Si and P. Uwer, “QCD corrected spin analyzing power of jets in decays of polarized top quarks,” *Phys. Lett. B* **539** (2002) 235.
- [8] M. Baumgart and B. Tweedie, “Transverse Top Quark Polarization and the  $t\bar{t}$  Forward-Backward Asymmetry,” *J. High Energy Phys.* **1308** (2013) 072.
- [9] W. Bernreuther, A. Brandenburg and P. Uwer, “Transverse polarization of top quark pairs at the Tevatron and the large hadron collider,” *Phys. Lett. B* **368** (1996) 153.
- [10] V. M. Abazov *et al.* (D0 Collaboration), “Measurement of Leptonic Asymmetries and Top Quark Polarization in  $t\bar{t}$  Production,” *Phys. Rev. D* **87**, 011103 (2013).
- [11] V. M. Abazov *et al.* (D0 Collaboration), “Simultaneous Measurement of Forward-Backward Asymmetry and Top Polarization in Dilepton Final States from  $t\bar{t}$  Production at the Tevatron,” submitted to *Phys. Rev. D*, arXiv:1507.05666 [hep-ex].
- [12] G. Aad *et al.* (ATLAS Collaboration), “Measurement of Top Quark Polarization in Top-Antitop Events from Proton-Proton Collisions at  $\sqrt{s} = 7\text{ TeV}$  Using the ATLAS Detector,” *Phys. Rev. Lett.* **111**, 232002 (2013).
- [13] S. Chatrchyan *et al.* (CMS Collaboration), “Measurements of  $t\bar{t}$  spin correlations and top-quark polarization using dilepton final states in  $pp$  collisions at  $\sqrt{s} = 7\text{ TeV}$ ,” *Phys. Rev. Lett.* **112**, 182001 (2014).
- [14] J. A. Aguilar-Saavedra, “Missing Top Properties.” In: Proceedings of the 7th International Workshop on Top Quark Physics, Cannes, France, 2014, edited by Frdric Derue, Stanford University, eConf C1409281.
- [15] W. Bernreuther, M. Fucker and Z. G. Si, “Weak interaction corrections to hadronic top quark pair production: Contributions from quark-gluon and b anti-b induced reactions,” *Phys. Rev. D* **78**, 017503 (2008); W. Bernreuther and Z. -G. Si, unpublished e-mail communication.
- [16] S. Fajfer, J. F. Kamenik and B. Melic, “Discerning New Physics in Top-Antitop Production using Top Spin Observables at Hadron Colliders,” *JHEP* **1208**, 114 (2012).
- [17] V. M. Abazov *et al.* (D0 Collaboration), “The Upgraded D0 Detector,” *Nucl. Instrum. Methods Phys. Res. Sec. A* **565**, 463 (2006).
- [18] R. Angstadt *et al.*, “The layer 0 inner silicon detector of the D0 experiment,” *Nucl. Instrum. Methods Phys. Res. Sec. A* **622**, 298 (2010).
- [19] S. Abachi *et al.* (D0 Collaboration), “The D0 Detector,” *Nucl. Instrum. Methods Phys. Res. A* **338**, 185 (1994).
- [20] V. M. Abazov *et al.* (D0 Collaboration), “The muon system of the Run II D0 detector,” *Nucl. Instrum. Methods Phys. Res. Sec. A* **552**, 372 (2005).
- [21] V. M. Abazov *et al.* (D0 Collaboration), “Electron and Photon Identification in the D0 Experiment,” *Nucl. Instrum. Meth. Phys. Res. Sec A* **750**, 78 (2014).
- [22] V. M. Abazov *et al.* (D0 Collaboration), “Muon reconstruction and identification with the Run II D0 detector,” *Nucl. Instrum. Methods Phys. Res. Sec. A* **737**, 281 (2014).
- [23] G. Blazey *et al.*, “Run II jet physics,” arXiv:hep-ex/0005012.
- [24] V. M. Abazov *et al.* (D0 Collaboration), “Jet energy scale determination in the D0 experiment,” *Nucl. Instrum. Methods Phys. Res. Sec. A* **763**, 442 (2014).
- [25] V. M. Abazov *et al.* (D0 Collaboration), “Improved  $b$  quark jet identification at the D0 experiment,” *Nucl. Instrum.*

Methods Phys. Res. Sec. A **763**, 290 (2014).

- [26] V. M. Abazov *et al.* (D0 Collaboration), “Measurement of differential  $t\bar{t}$  production cross sections in  $p\bar{p}$  collisions,” Phys. Rev. D **90**, 092006 (2014).
- [27] S. Frixione and B. R. Webber, “Matching NLO QCD computations and parton shower simulations,” JHEP **0206** (2002) 029; S. Frixione *et al.*, “Matching NLO QCD and parton showers in heavy flavour production,” JHEP **0308** (2003) 007.
- [28] M. L. Mangano, M. Moretti, F. Piccinini, R. Pittau and A. D. Polosa, “ALPGEN, a generator for hard multiparton processes in hadronic collisions,” JHEP **0307**, 001 (2003).
- [29] G. Corcella *et al.*, “HERWIG 6: An Event generator for hadron emission reactions with interfering gluons (including supersymmetric processes),” JHEP **0101**, 010 (2001).
- [30] T. Sjöstrand, S. Mrenna, and P. Skands, “PYTHIA 6.4 physics and manual,” J. High Energy Phys. 05 (2006) 026.
- [31] R. Brun and F. Carminati, CERN Program Library Long Writeup W5013 (1993) (unpublished).
- [32] E. Boos *et al.* [CompHEP Collaboration], “CompHEP 4.4: Automatic computations from Lagrangians to events,” Nucl. Instrum. Meth. A **534**, 250 (2004).
- [33] V. M. Abazov *et al.* (D0 Collaboration), “Measurement of the  $t\bar{t}$  production cross section in  $p\bar{p}$  collisions at  $\sqrt{s} = 1.96$  TeV using secondary vertex  $b$  tagging,” Phys. Rev. D **74**, 112004 (2006).
- [34] V. M. Abazov *et al.* (D0 Collaboration), “Measurement of the forward-backward asymmetry in top quark-antiquark production in  $p\bar{p}$  collisions using the lepton+jets channel,” Phys. Rev. D **90**, 072011 (2014).
- [35] R. Demina, A. Harel and D. Orbaker, “Reconstructing  $t\bar{t}$  events with one lost jet,” Nucl. Instrum. Methods Phys. Res. Sec. A **788**, 128 (2015).
- [36] W. Bernreuther, “Top quark physics at the LHC,” J. Phys. G **35**, 083001 (2008).
- [37] V. M. Abazov *et al.* (D0 Collaboration), “Measurement of the forward-backward asymmetry in the distribution of leptons in  $t\bar{t}$  events in the lepton+jets channel,” Phys. Rev. D **90**, 072001 (2014).
- [38] M. Czakon, P. Fiedler and A. Mitov, “Resolving the Tevatron top quark forward-backward asymmetry puzzle,” arXiv:1411.3007 [hep-ph].